Incorporation of the Model Drug Ubidecarenone into Solid Lipid Nanoparticles

Heike Bunjes,[1,3] Markus Drechsler,[1] Michel H. J. Koch,[2] and Kirsten Westesen[1]

Received November 2, 2000; accepted December 12, 2000

Purpose. The impact of drug incorporation on melt-homogenized tripalmitin nanoparticles is investigated with ubidecarenone as a model drug. The dispersions are studied with respect to their drug loading capacity, localization and physical state of the drug as well as to potential changes of the nanoparticle properties due to interactions between drug and triglyceride matrix.

Methods. The investigations were carried out using photon correlation spectroscopy, differential scanning calorimetry, synchrotron radiation X-ray diffraction, ultracentrifugation, and cryo- and freeze-fracture transmission electron microscopy.

Results. Ubidecarenone can be incorporated into the dispersions in concentrations higher than 50% of the dispersed phase. The drug is associated with the nanoparticles such that small drug amounts are bound tightly to the carrier matrix while excess drug adheres as a liquid phase to the crystalline particles. Drug incorporation lowers the crystallization and melting temperature of the particle matrix and accelerates the transition of the triglyceride into the stable β-polymorph after crystallization.

Conclusions. Drug incorporation may significantly alter important physicochemical parameters of solid lipid nanoparticles. Slow release of ubidecarenone may only be possible for the fraction of drug which is tightly bound to the matrix while the liquid fraction should be rapidly released.

KEY WORDS: solid lipid nanoparticles; ubidecarenone (coenzyme Q_{10}); drug loading; physicochemical characterization; electron microscopy.

INTRODUCTION

Nanoparticles based on solid lipids, e.g., triglycerides, have been proposed as novel drug carrier systems combining the advantages of colloidal lipid emulsions with those of particles with a solid matrix (1). Such lipid suspensions can be obtained by emulsification of the molten matrix lipid and subsequent recrystallization of the dispersed phase. This preparation technique makes it possible to use compositions which are exclusively based on physiological or physiologically acceptable compounds, thus avoiding toxicity problems often associated with the administration of polymeric nanoparticles: Polymer nanoparticles may contain residues of toxic monomers or solvents, be not or only slowly degradable or form toxic degradation products. The small size of triglyceride nanoparticles may allow their parenteral, in particular intravenous administration. Since they immobilize drugs more strongly than emulsions (2), they could serve as sustained release systems and be valuable carriers for drug targeting. Due to the lipophilic nature of their matrix, solid triglyceride nanoparticles are considered particularly useful for the administration of lipophilic drugs.

Hitherto, however, only limited information is available concerning the impact of drug incorporation on glyceride suspensions prepared by melt-homogenization (2–9). This point is of particular interest since drug incorporation may alter the ultrastructure of the dispersion, e.g., the particle size and shape or the physical state of the particles. Such alterations could influence pharmaceutical as well as pharmacokinetic parameters of the dispersions such as shelf life, biodistribution of the particles or drug release. Moreover, the physical state and localization of the incorporated drug is crucial for the *in vitro* and *in vivo* performance of the preparation. To evaluate the influence of drug incorporation on triglyceride nanoparticle dispersions the highly lipophilic, heart-protecting drug ubidecarenone (Coenzyme Q_{10}, Q_{10}) was chosen as a model for the present study. Q_{10}-loaded tripalmitin dispersions were investigated with respect to the drug loading capacity of the dispersions, the question if and to what extent Q_{10} is associated with the lipid suspension particles as well as its physical state and location within the system. Moreover, we were interested in potential changes of the nanoparticle properties, e.g., regarding particle size and shape, physical state and crystal structure as well as melting and crystallization behavior, due to interactions between drug and triglyceride matrix.

MATERIALS AND METHODS

Materials

Ubidecarenone (Q_{10}, Pharmacia AB, S-Uppsala; Kyowa Hakko Kogyo, J-Tokyo), tripalmitin (Dynasan 116, D16, Hüls AG, D-Witten), Lipoid S100 (S100, Lipoid KG, D-Ludwigshafen), sodium glycocholate (SGC, Sigma, USA-St. Louis), tyloxapol (Sterling Organics, USA-Rensselaer), glycerol 85% (Wasserfuhr, D-Bonn), thiomersal (Synopharm, D-Barsbüttel). Water was doubly distilled or purified by reverse osmosis (Alpha-Q, Millipore, D-Eschborn).

Preparation of Bulk Mixtures

Q_{10}-tripalmitin mixtures were prepared by mixing the two substances in the melt and subsequent cooling. Samples were first cold stored (4–8°C) to facilitate crystallization and subsequently equilibrated at room temperature.

Composition and Preparation of Dispersions

The dispersions consisted of 10% lipid phase (triglyceride plus Q_{10}) and either 2.4% S100 and 0.6% SGC (abbreviated as "PG") or 2% S100 and 2% tyloxapol ("PT") as stabilizer blends. The drug content of the lipid phase ranged from 2% to 90%. Samples without drug in or with 100% Q_{10} as the lipid phase were also prepared. The aqueous phase contained 0.01% thiomersal as a preservative and 2.25% glyc-

[1] Friedrich Schiller University Jena, Institute of Pharmacy, Department of Pharmaceutical Technology, Lessingstrasse 8, 07743 Jena, Germany.

[2] European Molecular Biology Laboratory, Hamburg Outstation, EMBL c/o DESY, Notkestrasse 85, 22603 Hamburg, Germany.

[3] To whom correspondence should be addressed. (e-mail: Heike.Bunjes@uni-jena.de)

0724-8741/01/0300-0287$19.50/0

erol. The dispersions were prepared in the heat (70–80°C). The phospholipid was dispersed in the molten triglyceride with or without ultrasonication until an optically clear liquid was obtained. The drug was added to the lipid phase. In some cases, the phospholipid was dispersed in the mixture of triglyceride and drug. The hot aqueous phase containing the hydrophilic surfactant was added and a predispersion was prepared by probe sonication. The predispersion was homogenized (Micron Lab 40, APV Gaulin, D-Lübeck) for 5 cycles at 800 bars. Except for the D16-Q-PG-3 series the dispersions were filtered (0.45 μm) and the systems were allowed to cool to room temperature. Samples were stored at room (20–25°C) and at refrigerator temperature (4–8°C). Unless otherwise specified, experimental data were obtained on cold stored samples.

Sample names follow the convention "matrix triglyceride-Q(Q_{10} concentration within lipid phase)-stabilizer composition-batch": A sample denoted D16-Q(10)-PG-1, for example, contains a lipid phase consisting of 90% tripalmitin and 10% Q_{10}, is stabilized with the S100/SGC mixture and has the batch number 1. Information on drug concentration always refers to the drug load of the lipid phase.

Photon Correlation Spectroscopy (PCS)

An estimate of the mean particle size was obtained by PCS at 90° (Zetasizer 3, Malvern, D-Herrsching; BI Zetaplus, Brookhaven Instruments Corporation, USA-Holtsville). The dispersions were diluted with demineralized, filtered water to an appropriate scattering intensity. Data was analyzed by the cumulants method assuming spherical particle shape. Accordingly, the results are given as the effective diameter (often also called z-average diameter) and the polydispersity index (PI) as a parameter for the width of the particle size distribution (for an ideally monodisperse system, the theoretical PI would be 0). Under certain conditions, cumulant parameters can be related to those of common size distribution functions (see, e.g., (10).

Differential Scanning Calorimetry (DSC)

Samples were investigated in a DSC 2, DSC 7 or Pyris 1 DSC (Perkin Elmer, D-Überlingen) at different scan rates. The sample weight for the dispersions was around 10–20 mg. The quantity of bulk samples was adjusted to approximately the same amount as present in the dispersions. For investigation in a Micro DSC III (Setaram, F-Caluire) about 150–160 mg of dispersion were used.

Synchrotron Radiation X-Ray Diffraction

Measurements were performed on the double focusing monochromator mirror camera X33 of the EMBL in HASYLAB on the storage ring DORIS III of the Deutsches Elektronen Synchrotron (DESY) at Hamburg, Germany, as described previously (5). The scattering pattern of the particles was recorded at 20°C in three separate 1 min time frames. For recrystallization studies, the nanoparticles were held around 20–25°C above their melting temperature for at least 10 min and then rapidly cooled to at least 5°C above the expected onset of crystallization. Further cooling was performed at about 0.31°C/min and the scattering pattern was monitored continuously in 1 min time frames.

Ultracentrifugation

The undiluted dispersions D16-Q(0)-PG-1, D16-Q(10)-PG-1, D16-Q(0)-PG-1 (stored for more than 1.5 years), D16-Q(50)-PG-2, D16-Q(50)-PT (stored for more than 4 months) and Q(100)-PT (stored for 2 days) were centrifuged (L8-55 ultracentrifuge, rotor SW 55 Ti, Beckman Instruments, D-München) for six hours at 35000 rpm (corresponding to approx. 116000 × g).

Transmission Electron Microscopy of Freeze-Fractured Specimen

Samples were freeze-fractured at about –150°C and 10^{-7} to 10^{-6} mbar (BAF 060, Bal-Tec, FL-Balzers) after jet freezing as a thin film with liquid propane (JFD-030, Bal-Tec, FL-Balzers). Shadowing was performed with platinum/carbon at 45° and replica were stabilized by vertical deposition of pure carbon. After cleaning with a methanol-chloroform mixture (1:1), the replicas were viewed in a transmission electron microscope (CEM 902A, Zeiss, D-Oberkochen), operated at 80°kV.

Cryo-Transmission Electron Microscopy

A drop of diluted dispersion was placed on an uncoated copper grid and excess liquid removed by blotting with a piece of filter paper. The sample was cryo-fixed by injection into liquid ethane cooled to about –180°C. Excess ethane was removed by blotting in the cold (11). The sample was transferred with a cryo-transfer-unit into a pre-cooled cryoelectron microscope (CEM 902A, Zeiss, Oberkochen) operated at 80 kV. Samples were viewed under low-dose conditions (beam current around 1μA resulting in a cumulative specimen dose of about 0.1 C/cm^2 at a primary magnification of 30000× (12)) at a constant temperature around 80 K.

RESULTS

Particle Size Analysis

The PCS effective diameters of the dispersions are between around 110 and 200 nm, with PIs being approximately in the range of those observed for commercial parenteral emulsions (Table I). Only minor changes of the particle size are observed upon storage or—except for the PT-stabilized dispersions—as a result of drug incorporation. The cause of the particle size differences between dispersions of the same composition (e.g., between the three D16-Q(0)-PG batches) could not exactly be clarified. Tentatively, the differences might be due to slight process variations.

DSC

In the bulk mixtures, two melting events pointing to the coexistence of a tripalmitin- and a Q_{10}-rich phase are detected (Fig. 1). In contrast, heating curves of dispersions usually display a single broad melting endotherm (Fig. 2) which often - in particular with the PT-stabilized systems - contains several side maxima or shoulders. The system with 70% Q_{10} seems to display several diffuse transitions upon heating which are, however, difficult to evaluate due to their low heat of transition. The peak temperature of the melting endotherm de-

Table I. PCS Particle Size (Effective Diameter) and Polydispersity Index (PI) of the Nanodispersions

	After preparation[a] size (nm)/PI	After long term storage[b] size (nm)/PI
D16-Q(0)-PG-1	148/0.17	149/0.25
D16-Q(10)-PG-1	139/0.18	144/0.19
D16-Q(20)-PG-1	149/0.17	158/0.16
D16-Q(30)-PG-1	147/0.19	154/0.13
D16-Q(50)-PG-1	153/0.19	159/0.15
D16-Q(0)-PG-2	175/0.16	169/0.20
D16-Q(5)-PG-2	151/0.14	157/0.15
D16-Q(10)-PG-2	154/0.17	155/0.12
D16-Q(30)-PG-2	172/0.13	169/0.18
D16-Q(50)-PG-2	163/0.13	158/0.23
D16-Q(70)-PG-2	172/0.18	182/0.14
D16-Q(90)-PG-2	178/0.13	185/0.14
D16-Q(0)-PG-3		194/0.16
D16-Q(2)-PG-3		197/0.16
D16-Q(4)-PG-3		180/0.14
D16-Q(6)-PG-3		196/0.15
D16-Q(8)-PG-3		187/0.15
D16-Q(10)-PG-3		184/0.16
D16-Q(0)-PT	178/0.22	164/0.21
D16-Q(10)-PT	114/0.20	109/0.26
D16-Q(30)-PT	108/0.20	121/0.14
D16-Q(50)-PT	122/0.20	154/0.18
Q(100)-PT	167/0.20[c]	

[a] Samples were measured within one day after preparation (storage at room temperature).
[b] Long-term cold storage: More than 4 years for D16-Q-PG-1 dispersions, almost 3 years for D16-Q-PG-2 and D16-Q-PT-dispersions, more than 6 months for D16-Q-PG-3 dispersions.
[c] Cold stored sample.

creases with increasing drug load. The transition temperature suggests that the endotherm is due to the melting of tripalmitin. For dispersions with higher drug load the heat of transition is lower than expected for completely crystalline particles. Heat of transitions normalized on tripalmitin content tend to decrease with increasing drug load. The crystallization temperature also decreases with increasing drug concentration (Fig. 3). Since the crystallization temperature of particles with higher drug load is below room or refrigerator temperature crystallization of the nanoparticles is retarded or even prevented upon storage at these temperatures. In the dispersion D16-Q(50)-PG-2, for example, less than 3% of the triglyceride (related to the bulk material used for preparation) has crystallized after almost three years of storage at room temperature. When this dispersion is investigated in temperature cycles no increase in melting or crystallization temperatures is observed with increasing cycle number. The depression of melting and crystallization temperatures is still observed after long-term storage (Fig. 3). After long-term storage of PG-stabilized dispersions loaded with 20% and more drug a pretransition is observed prior to the main crystallization endotherm. Comparison with the recrystallization temperatures in a series of nanoparticles loaded with low amounts of Q_{10} (D16-Q-PG-3) reveals that the onset temperature of the pretransition is comparable to that expected for a 6 to 8% drug load (Fig. 3). In some of the dispersions displaying a pretransition upon crystallization there is also a small additional melting transition (slightly above 60°C) after the main endotherm upon heating. These alterations, which were not observed after one year of storage in the D16-Q-PG-1 series occur in different intensity in the two different series of PG-stabilized dispersions. In PT-stabilized dispersions they are not observed at all within 3 years of storage.

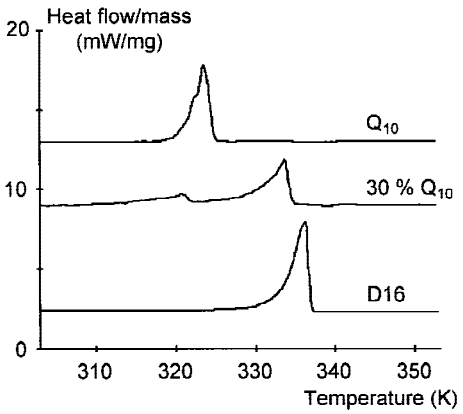

Fig. 1. DSC heating curves of bulk samples (untreated raw materials of Q_{10} and D16, and a mixture of 30% Q_{10} and 70% D16 crystallized from the melt (30% Q_{10})).

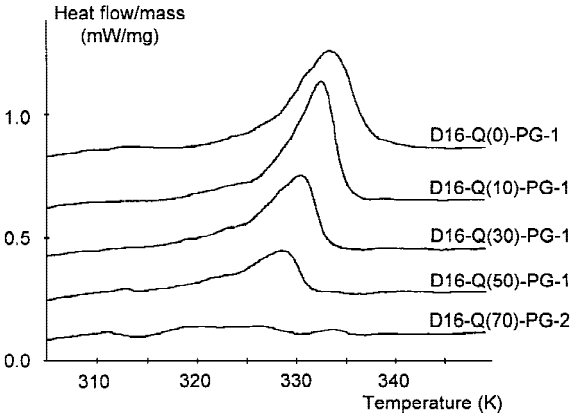

Fig. 2. DSC heating curves of Q_{10}-loaded tripalmitin dispersions (cold stored for 7 months, D16-Q(70)-PG-2: 5.5 months). The curves are displaced along the ordinate for better visualization.

X-Ray Diffraction

The X-ray diffractograms of the bulk mixtures contain reflections due to crystalline drug beside those of the β-form of tripalmitin (Fig. 4). In contrast, drug-loaded dispersions display only the diffraction pattern of the stable β-polymorph of tripalmitin but no reflections characteristic of Q_{10} (Fig. 5). The positions of the peak maxima do not change noticeably with increasing drug load. Due to an asymmetry of the small angle reflection, however, its mean position is shifted to slightly smaller angles for drug-loaded dispersions. Depending on their thermal history, dispersions with high drug load do not display any reflections (cold stored dispersion loaded with 90% drug; dispersions stored at room temperature loaded with 50% and more Q_{10}). The small angle reflection intensity normalized on tripalmitin content of the dispersions decreases with increasing drug load. The line width of the small angle reflection of PG- (but not of PT-) stabilized drug

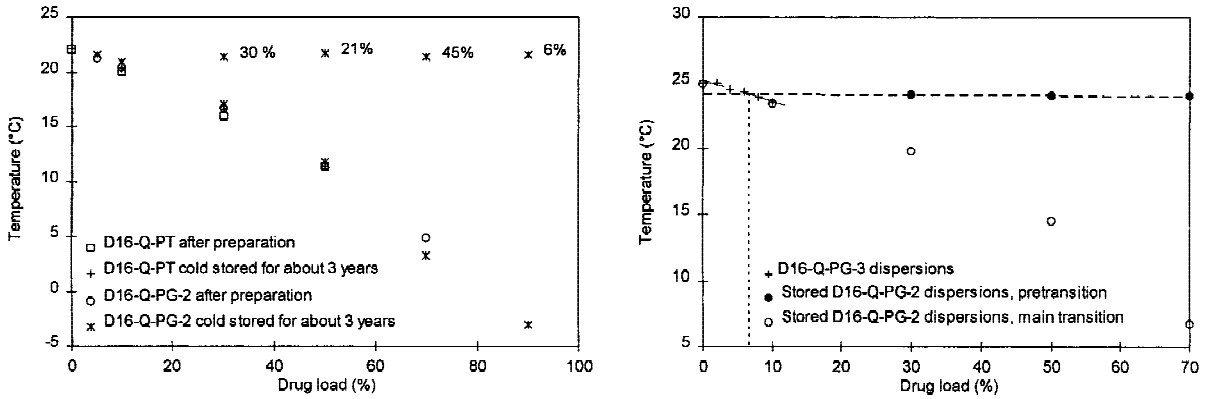

Fig. 3. Crystallization temperatures of fresh and long-term stored Q_{10}-loaded dispersions (left, 5°C/min., T_{onset}; the values beside the data points give the approximate fraction of heat of transition related to the whole crystallization exotherm) and comparison of the pretransition temperature of long-term stored PG-dispersions with the crystallization temperature of dispersions with low drug load (right, 0.05°C/min., T_{onset}).

loaded dispersions is significantly reduced compared to the unloaded reference sample. In the dispersions loaded with low amounts of Q_{10} (D16-Q-PG-3), the line width decreases with increasing drug load up to a concentration of 6% Q_{10} and then remains constant at higher drug loads. A similar decrease of wide angle line widths could not be observed.

In recrystallization studies on selected PG-stabilized systems pronounced differences in transition kinetics are observed between drug loaded and drug free dispersions (Fig. 6). While crystallization of unloaded carrier suspension particles proceeds *via* the α-modification which is the usual way for triglyceride crystallization from the melt, the Q_{10}-loaded dispersions hardly display any reflections of the α-modification upon crystallization. Only the dispersion loaded with 5% Q_{10} still displays distinct α-reflections beside simultaneously appearing β-reflections but the transition still proceeds faster than in the unloaded dispersion.

Ultracentrifugation

Particles in dispersions without or with only 10% Q_{10} undergo sedimentation. In contrast, dispersions with 30% and more Q_{10} as well as a dispersion of pure Q_{10} cream and form a solid phase as the top layer (the triglyceride-containing dispersions also displaying a slight sediment).

Electron Microscopy

In cryoelectron microscopy, tripalmitin nanoparticles loaded with 10% Q_{10} (Fig. 7a) appear as platelets which resemble those in unloaded tripalmitin dispersions (1). In dispersions loaded with 30 and 50% Q_{10}, the particles consist of a platelet-like basis with a cap of different contrast positioned on one side of each platelet (Fig. 7b). This two-phase structure can also be detected in a freeze-fracture specimen (Fig. 7c). The caps show a cauliflower-like surface structure which can also be detected on the surface and the rims of some platelets. Tentatively, these structures might be correlated with the dark appearance of the rims of the platelets and the blurred, dotted edges of the darker caps in the cryoelectron micrographs but this fine structure of the nanoparticles requires further investigation. Vesicular structures or emulsion droplets of supercooled melts which might be regarded as

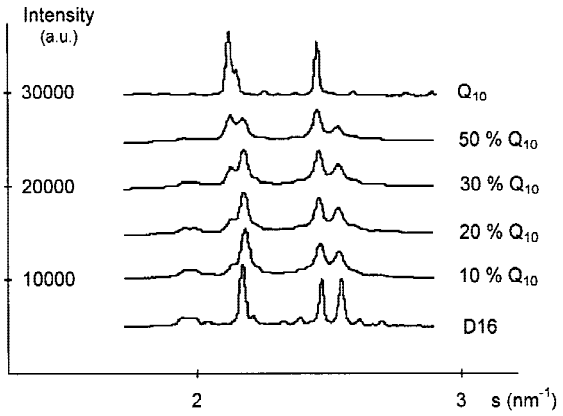

Fig. 4. Wide angle X-ray diffractograms of bulk mixtures containing the denoted amounts of Q_{10} and thermally untreated raw materials ($s = 2 \sin \Theta / \lambda$; 2Θ: scattering angle; λ: wavelength (appr. 0.15 nm)). The curves are displaced along the ordinate.

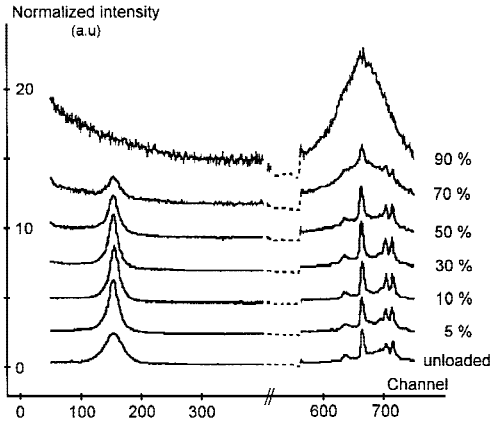

Fig. 5. Simultaneous small and wide angle X-ray diffractograms of Q_{10}-loaded, cold stored D16-Q-PG-2 dispersions. The diffractograms are normalized on triglyceride content and are displaced along the ordinate. The first order of tripalmitin in the small angle pattern (left panel) is at approximately 0.25 nm^{-1}; for the spacings of the wide angle reflections see Fig. 6.

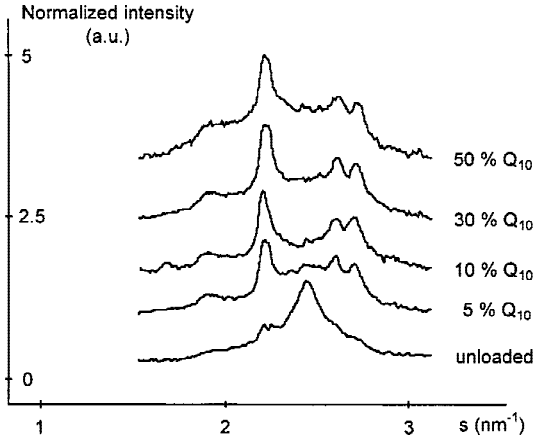

Fig. 6. Wide angle X-ray diffractograms of D16-Q-PG-2 dispersions approximately 4 min. after the onset of crystallization. The diffractograms are normalized on triglyceride content and displaced along the ordinate. The diffractogram of the nanoparticles loaded with 10% Q_{10} is on a slightly different scale.

alternative localizations of Q_{10} could not be observed in the electron micrographs.

DISCUSSION

In contrast to other lipophilic drugs (2) Q_{10} can be incorporated into triglyceride nanosuspensions even in high concentrations. The results from DSC and X-ray investigations suggest that - in contrast to the bulk samples - nanoparticles in Q_{10}-loaded dispersions contain only one solid phase consisting mainly of crystalline tripalmitin. A crystalline Q_{10} phase was not detected in the dispersions. This result is in agreement with earlier results on melt-homogenized, colloidal dispersions of pure Q_{10} which display a high tendency towards the formation of emulsified supercooled melts instead of forming suspension particles (13,14). NMR investigations on Q_{10}-loaded trimyristin suspensions have revealed a liquid-like state of a significant Q_{10} fraction when the drug was incorporated in higher concentrations (2).

The decrease in melting and crystallization temperature of the matrix lipid with increasing drug concentration points to a concentration dependent association of Q_{10} with the nanoparticles resulting in eutectic behavior. The crystallization temperature of particles with high drug load is so low that these particles do not crystallize but remain in the form of emulsified supercooled melts when stored at room temperature. Since no increase in transition temperature is observed in temperature cycles, which would be expected if separation of drug and matrix material into distinct particles occurred, the drug seems to have a high affinity for the nanoparticles. Transition temperatures display at most minor changes with time indicating that the drug remains bound during long-term storage.

The acceleration of polymorphic transitions upon crystallization of drug loaded dispersions also points to an association between carrier material and drug. A similar effect was observed in bulk mixtures which also transform into the stable triglyceride modification much faster than pure tripalmitin (data not shown). The effect on the transition kinetics can only be explained by an intimate interaction of the drug molecules with those of the triglyceride leading to an orientation of the triglyceride chains favoring the β-polymorph. This interaction is, however, not necessarily due to incorporation of the drug into the crystal lattice. An influence on transformation kinetics can also result from, e.g., interactions at the particle interface (15). The liquid state of Q_{10} in the particles is probably a main factor for the alteration of the transition kinetics. For hard fat suppository masses, the addition of lipophilic liquids induces a concentration dependent acceleration of the transition (16). The liquid phase was assumed to act as a solvent for the triglycerides in these systems, enabling their recrystallization into a more stable modification. A similar behavior may be possible for Q_{10}-loaded triglyceride nanoparticles. This assumption is supported by the fact that with increasing drug load not all of the triglyceride crystallizes as indicated by X-ray reflection intensities and crystallization enthalpy. The undetectable fraction of the triglyceride is presumably dissolved in the liquid Q_{10}. For dispersions with high drug load, in particular, a direct crystallization into the stable polymorph may also be possible since crystallization from solvents preferably occurs into the stable β-form (17). For low drug loads, the contamination of the lipid crystals with Q_{10} might enhance the mobility of the triglyceride molecules and destabilize the α-phase.

The ultrastructure of the drug loaded dispersions is revealed by electron microscopic studies. Nanoparticles loaded with higher amounts of Q_{10} consist of two different structures: The crystalline triglyceride forms characteristic platelets while excess drug remains liquid, forming a cap on one of the two large (001) faces of the platelet. A large fraction of the drug is obviously expelled from the triglyceride matrix upon crystallization as a liquid and a kind of two-phase particle is formed. Even in the presence of a crystalline triglyceride matrix the supercooling obtained on cold storage is obviously not sufficient to induce nucleation of Q_{10} in the lipid particles. The localization of the drug on one side of the particle seems to be energetically favorable compared to an even distribution of the drug over the whole particle surface. Dispersions loaded with only minor amounts of drug do not exhibit caps of excess drug. This result is in agreement with results from earlier ^{1}H NMR experiments on drug loaded trimyristin particles revealing that very little if any liquid drug is present in suspensions with lower drug load (2). The interpretation of the electron microscopic data is also supported by the results of the ultracentrifugation experiments. The observed decrease in particle density with increasing drug load can be explained by the increasing amount of liquid drug adhering to the solid particle matrix.

Since the liquid caps become increasingly difficult to detect with decreasing drug load, they can hardly be utilized to estimate the saturation limit of the triglyceride particles. The emulsifier dependent phase separation of triglyceride from the nanoparticles which is observed upon long-term storage of PG-stabilized dispersions with higher drug-load may give some additional information on this aspect. The tendency towards phase separation of tripalmitin obviously depends on the type of stabilizer since it is not observed in PT-stabilized dispersions. The mechanism of phase separation has not yet been identified. The crystallization temperature of the phase separated triglyceride is slightly below that of the raw material due to its association with drug molecules. Assuming saturation of the phase separated tripalmitin with Q_{10}, the saturation limit of the tripalmitin matrix can be estimated by com-

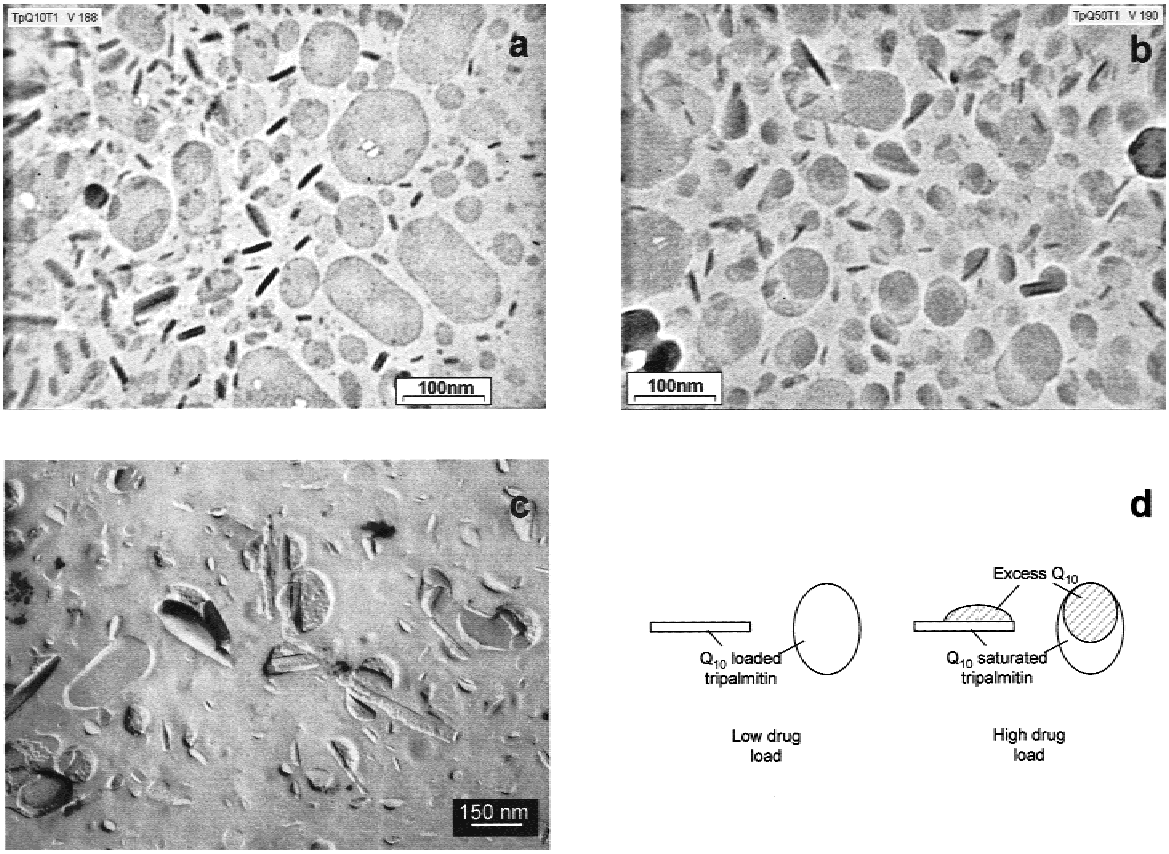

Fig. 7. Cryo-transmission electron micrographs of the dispersion D16-Q(10)-PT (a) and the dispersion D16-Q(50)-PT (b); electron micrograph of a freeze-fractured specimen of the sample D16-Q(50)-PT (c); sketch of the particle structures (d).

parison with reference dispersions with low drug-load to be approximately 6 to 8% Q_{10}. Conclusions drawn from such a comparison must, however, be interpreted with caution, since the differences in crystallization temperature are small and the crystallization temperature is not solely influenced by the drug content but is, for instance, also dependent on particle size (18). The conclusion of a saturation limit around 6% Q_{10} for tripalmitin nanoparticles is supported by the fact that this is also the concentration range where no further decrease of small angle X-ray reflection line width takes place in the dispersions with low drug load. This decrease in line width observed in the Q_{10}-loaded PG-dispersions could, in principle, result from an increasing number of repeating units in the crystal lattice (perpendicular to the (001) planes) or a decrease in mosaicity in this direction. The latter possibility seems improbable for particles that are "contaminated" with drug molecules. An increase in the number of layers would only be possible *via* a change in particle shape since no increase in overall particle size is observed in PCS.

Concerning drug localization within the dispersion, the following conclusions can be drawn: A small portion of drug is associated with the triglyceride matrix in such a way that - according to NMR results (2) - the mobility of the drug molecules is highly restricted. The immobilization may result from the incorporation of drug molecules into the crystal structure. A rigid adsorption of the drug molecules to the particle surface can, however, also not be excluded. The excess drug which cannot be immobilized by the triglyceride is expelled from the carrier matrix upon crystallization and adheres as a liquid phase to the platelet surface. It thereby remains associated with the lipid nanoparticles due to its liquid state in combination with appropriate wetting properties. This behavior is in contrast to observations on other lipophilic drugs which tend to form a separate phase in the dispersion after expulsion from the lipid matrix (2). In these cases, the incorporated drugs are probably unable to form a wetting liquid on the triglyceride particles after expulsion from the matrix and will crystallize. A crystalline, solid phase will, however, only in very few cases have properties allowing its strong adherence to the particle surface and will thus separate from the carrier particles. The ability of a drug to be associated with the nanoparticles in a liquid state might thus be a general advantage or even a prerequisite for a stable binding of larger drug amounts to solid lipid nanoparticles, provided that the carrier particles are adequately wetted by the liquid drug. Localization of the drug, particularly in a liquid state, at the particle surface is, however, not supposed to lead to the desired sustained or controlled drug release which can only be expected for a drug incorporated into the lipid matrix. A modified release can thus only be assumed for particles with a Q_{10} load below the saturation limit of the triglyceride matrix. Since Q_{10} displays a rather uncommon behavior with its tendency to form stable supercooled melts in the colloidal state the results obtained on this drug should be transferred to other systems only with caution.

CONCLUSIONS

As obvious from the investigations of Q_{10} loaded tripalmitin dispersions drug incorporation may have pronounced effects on the physicochemical behavior of the carrier particles in terms of melting and crystallization behavior as well as kinetics of polymorphic transitions of the triglyceride. Higher concentrations of drug can completely prevent the formation of solid particles by the large depression of the crystallization temperature. Such alterations must be taken into account upon development of appropriate drug-loaded formulations.

The model drug ubidecarenone can be associated with tripalmitin nanoparticles in high concentrations. Immobilization of the drug molecules by the triglyceride lattice allowing sustained release may, however, only be possible at comparatively low concentrations since larger amounts of Q_{10} are not taken up by the triglyceride crystals but adhere to them as a separate liquid phase from which rapid release is expected. If modified release is not the major point of interest but solubilization of poorly soluble drugs is required, the processing into dispersions of supercooled melts (13,14) may be more advantageous for substances with high supercooling tendency, as they can hold larger amounts of drug due to the absence of a carrier and require less complex composed stabilizers.

ACKNOWLEDGMENTS

The authors thank S. Richter for assistance during the freeze-fracture electron microscopic investigations, Mrs. Buchta for the support during the ultracentrifugation experiments, and S. Liedtke for the help with sample preparation. H.B. and K.W. thank Pharmacia & Upjohn for financial support of parts of the work.

REFERENCES

1. K. Westesen and B. Siekmann. Biodegradable colloidal drug carrier systems based on solid lipids. In S. Benita (ed.), *Microencapsulation,* Marcel Dekker, New York, 1996 pp. 213–258.
2. K. Westesen, H. Bunjes, and M. H. J. Koch. Physicochemical characterization of lipid nanoparticles and evaluation of their drug loading capacity and sustained release potential. *J. Control. Release* **48**:223–236 (1997).
3. K. Westesen, B. Siekmann, and M. H. J. Koch. Investigations on the physical state of lipid nanoparticles by synchrotron radiation X-ray diffraction. *Int. J. Pharm.* **93**:189–199 (1993).
4. B. Siekmann and K. Westesen. Thermoanalysis of the recrystallization process of melt-homogenized glyceride nanoparticles. *Colloids Surfaces B: Biointerfaces* **3**:159–175 (1994).
5. H. Bunjes, K. Westesen, and M. H. J. Koch. Crystallization tendency and polymorphic transitions in triglyceride nanoparticles. *Int. J. Pharm.* **129**:159–173 (1996).
6. C. Schwarz and W. Mehnert. Freeze drying of drug-free and drug-loaded solid lipid nanoparticles (SLN). *Int. J. Pharm.* **157**: 171–179 (1997).
7. A. zur Mühlen, C. Schwarz, and W. Mehnert. Solid lipid nanoparticles (SLN) for controlled drug delivery—Drug release and release mechanism. *Eur. J. Pharm. Biopharm.* **45**:149–155 (1998).
8. A. zur Mühlen and W. Mehnert. Drug release and release mechanism of prednisolone loaded solid lipid nanoparticles. *Pharmazie* **53**:552–555 (1998).
9. A. zur Mühlen, E. zur Mühlen, H. Niehus, and W. Mehnert. Atomic force microscopy studies of solid lipid nanoparticles. *Pharm. Res.* **13**:1411–1416 (1996).
10. J. C. Thomas. The determination of log normal particle size distributions by dynamic light scattering. *J. Colloid Interface Sci.* **117**:187–192 (1987).
11. M. C. Schmidtgen, M. Drechsler, J. Lasch, and R. Schubert. Energy-filtered cryotransmission electron microscopy of liposomes prepared from human stratum corneum lipids. *J. Microsc.* **191**: 177–186 (1996).
12. M. Drechsler and H.-J. Cantow. EELS data acquisition processing and display for the Zeiss CEM 902 based on Lotus 1-2-3: Application examples from a biological system and inorganic transition metal compounds. *J. Microsc.* **162**:61–76 (1991).
13. B. Siekmann and K. Westesen. Preparation and physicochemical characterization of aqueous dispersions of coenzyme Q_{10} nanoparticles. *Pharm. Res.* **12**:201–208 (1995).
14. H. Bunjes, B. Siekmann, and K. Westesen. Emulsions of supercooled melts—A novel drug delivery system. In S. Benita (ed.), *Submicron Emulsions in Drug Targeting and Delivery,* Harwood Academic Publishers, Switzerland, 1998 pp. 175–204.
15. H. Bunjes and K. Westesen. Influences of colloidal state on physical properties of solid fats. In N. Garti and K. Sato (eds.) *Crystallization Process in Fats and Lipid Systems,* Marcel Dekker, New York, in press.
16. H. Yoshino, M. Kobayashi, and M. Samejima. Influence of the liquid phase coexisting in fatty suppository bases on the polymorphic transition rate. *Chem. Pharm. Bull.* **30**:2941–2950 (1982).
17. D. Chapman. The polymorphism of glycerides. *Chem. Rev.* **62**: 433–456 (1962).
18. H. Bunjes, M. H. J. Koch, and K. Westesen. Effect of particle size on colloidal solid triglycerides. *Langmuir* **16**:5234–5241 (2000).